Supporting Information – Testing Mantle Convection Simulations with Paleobiology and Other Stratigraphic Observations: Examples from Western North America

Victoria M. Fernandes[1,2], Gareth G. Roberts[2], Fred Richards[2]

[1]GFZ Potsdam, Helmholtz Zentrum, Telegrafenberg, 14473 Potsdam, Germany
[2]Department of Earth Science and Engineering, Imperial College London, South Kensington Campus, SW7 2AZ, UK.

Supplementary Figures

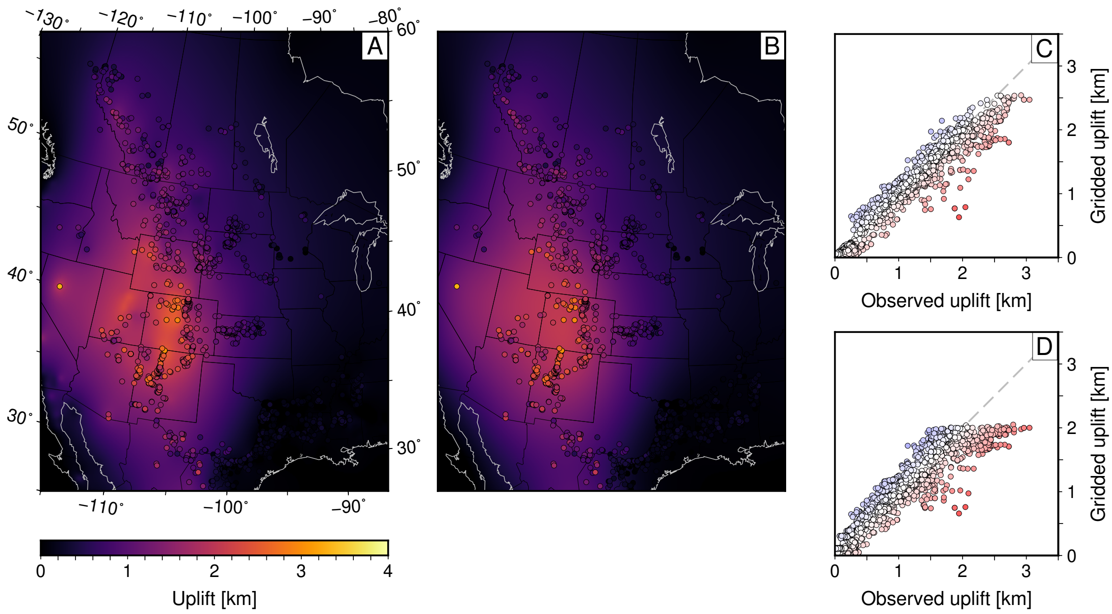

Figure S1. Gridded uplift data. A grid, with resolution 0.1°×0.1°, was generated by fitting splines with a tension factor of 1 to PBDB data (circles; see Figure 1 of main manuscript). In these examples, only PBDB data with paleo-water depth errors smaller than 1 km and stratigraphic markers of the last marine to non-marine transition are used in the gridding. The resulting grid was subsequently filtered using (A) 100 km and (B) 1000 km Gaussian low-pass filters. (C) Observed uplift from the stratigraphic record compared to uplift from the 100 km filtered grid, and (D) 1000 km filtered grid.

Corresponding author: V.M. Fernandes & G.G. Roberts, `milanez@gfz-potsdam.de`, `gareth.roberts@imperial.ac.uk`

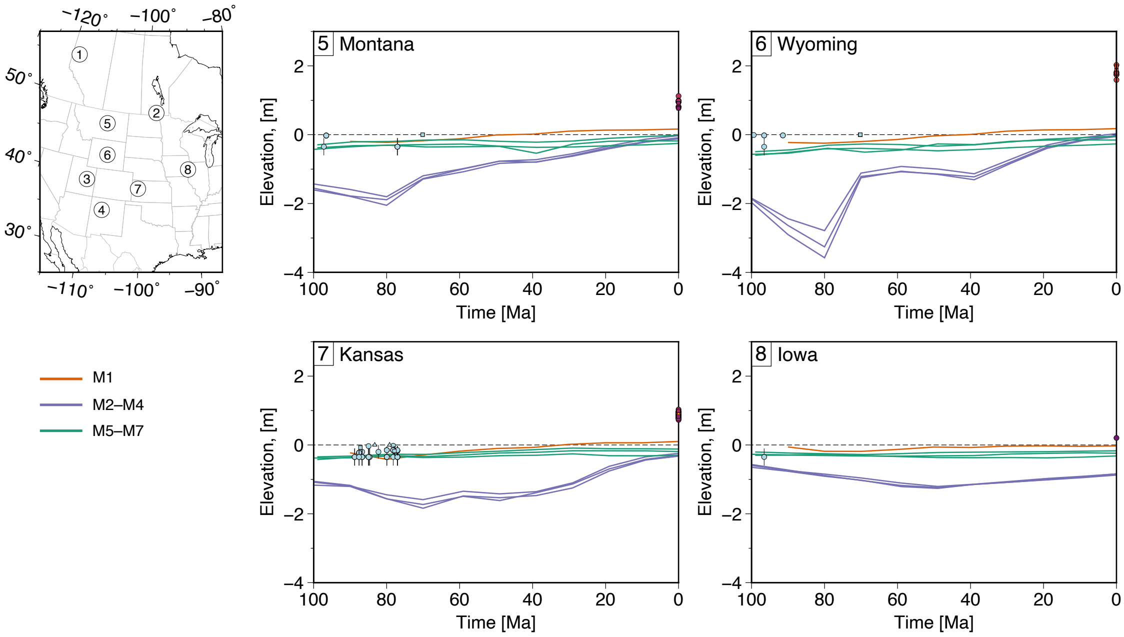

Figure S2. Uplift histories from stratigraphic observations compared to predicted dynamic topography at additional localities. Location map shows key locations of uplift histories shown in adjacent panels. (5-8) Circles = uplift measurements within 50 km of localities labelled in panel A. Error bars = paleo-water depth uncertainties. Coloured lines = dynamic topography histories predicted by ?: Orange = predictions from their model M1; purple = M2–4; green = M5–7 (see Figure 3 of main manuscript for extended description).

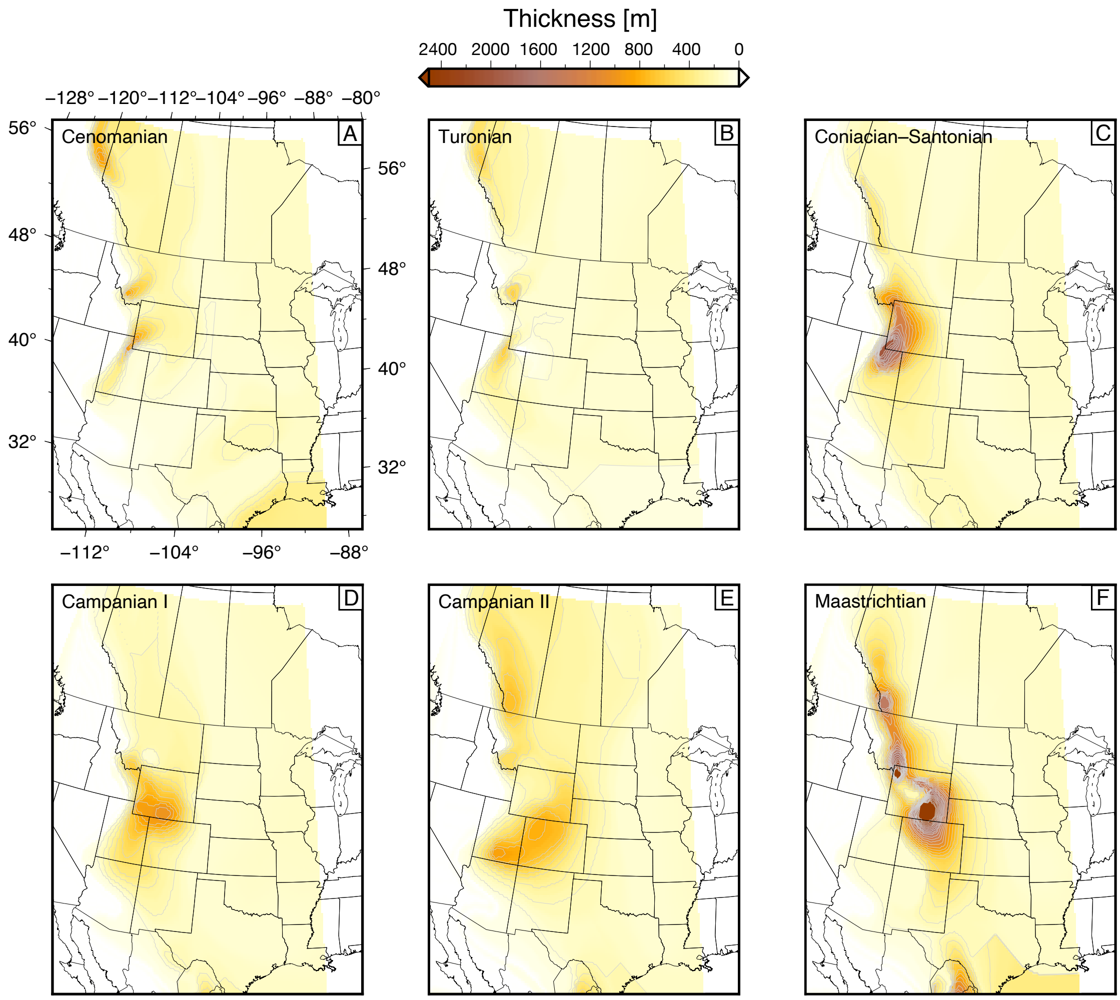

Figure S3. Isopach maps of the North American Western Interior from ?. These maps were used to estimate Upper Cretaceous subsidence patterns shown in Figure 5 of the main manuscript. Reconstructions are based on interpolation of rock outcrop and well data; control points are shown in their publication. Note that the isopachs have not been decompacted.

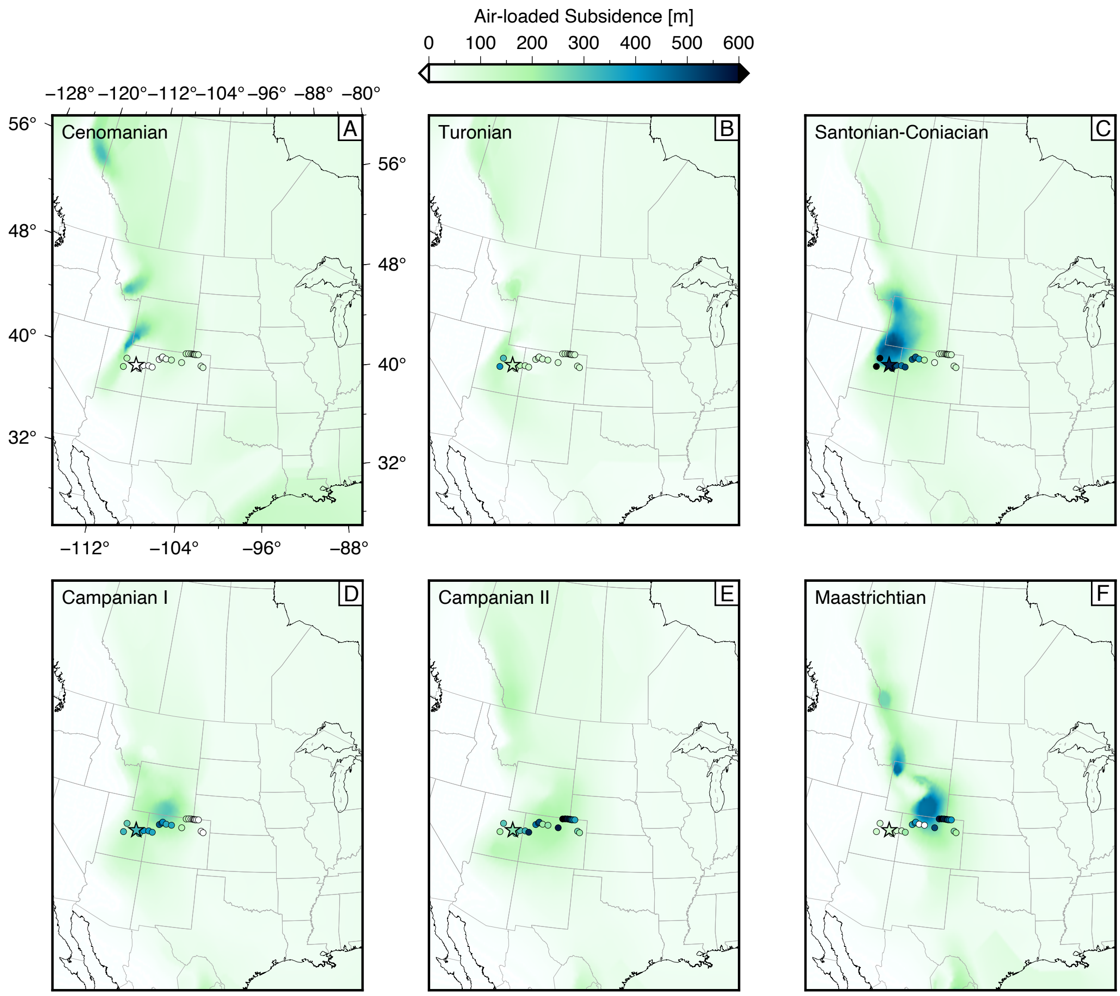

Figure S4. Late Cretaceous air-loaded subsidence by stage. Subsidence grids were generated by backstripping, decompacting and air-loading the isopach maps from **?** shown in Figure S3 of this document (see body text of main manuscript for details). Coloured circles = air-loaded subsidence from wells presented in **?**. Star = location of subsidence curve shown in Figure **??**. See body text of main manuscript for extended methodology.

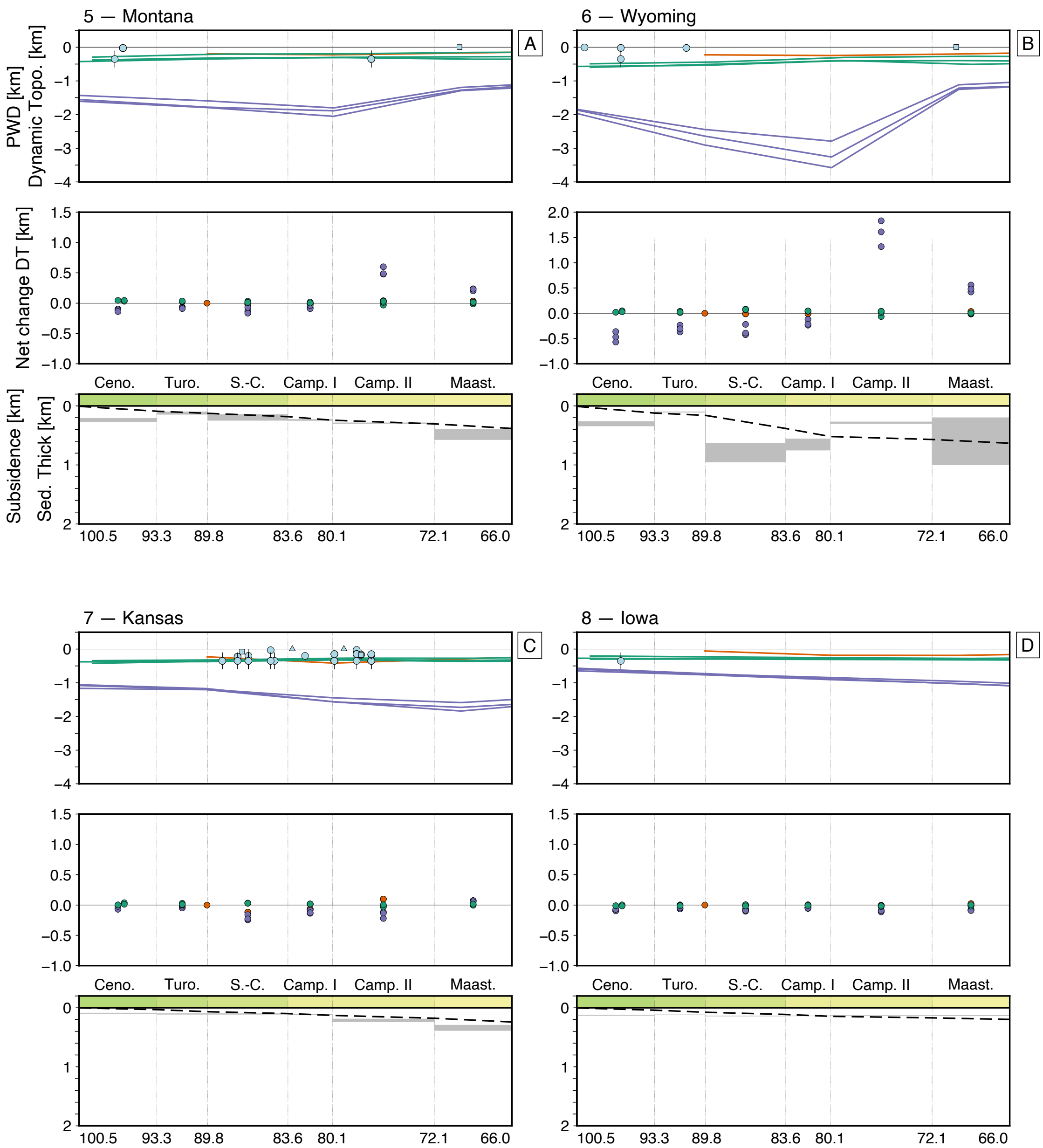

Figure S5. Comparison of predicted Late Cretaceous dynamic topography and independent subsidence histories. Predictions of dynamic topography, net change in dynamic topography per time interval and air-loaded subsidence for key locations 5–8 (Montana, Wyoming, Kansas and Iowa). See Figure S2 for locations and Figure **??** of main text for full description.

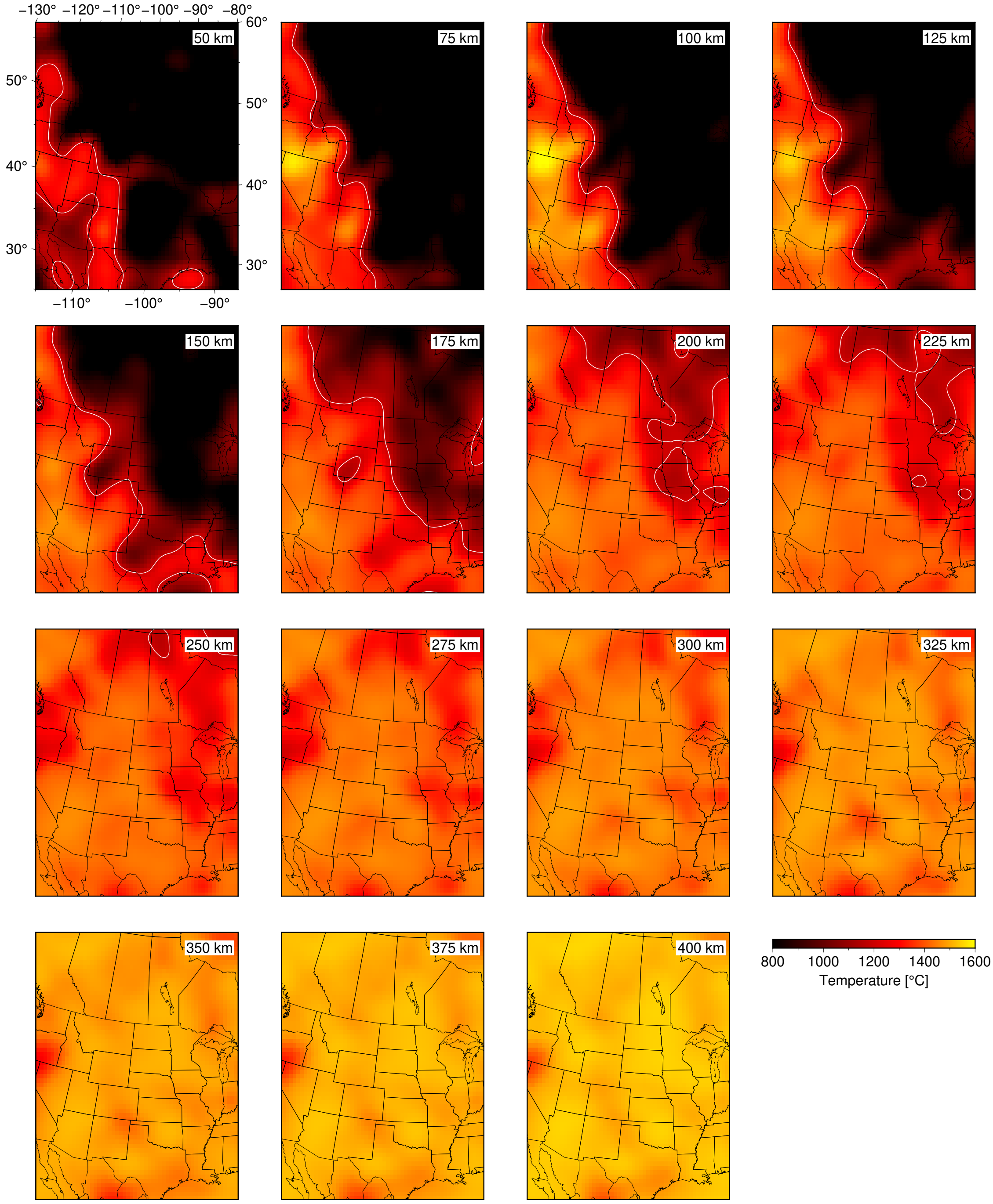

Figure S6. Calculated upper mantle temperatures. Temperature grids were generated by converting **?**'s V_s model–a version of **?**'s model that includes an update for North America, and **?**'s models for the South Atlantic Ocean and Africa. Solid white line = 1200°C isotherms at each labelled depth. These grids were used to generate the lithospheric thickness map and cross sections shown and discussed in relation to Figures 7–8 of the main manuscript.

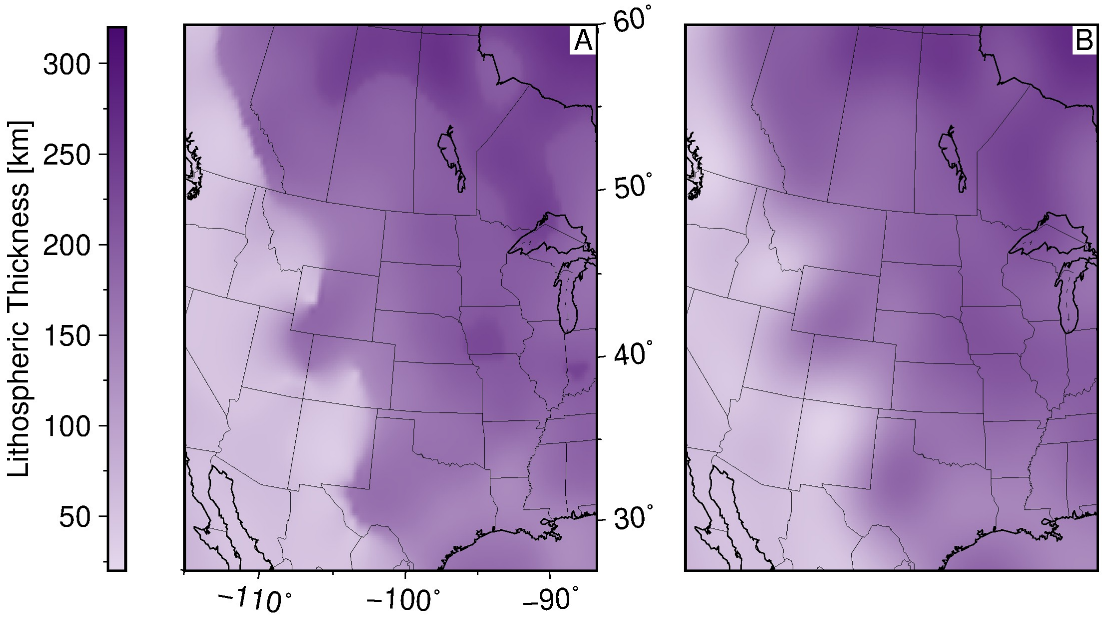

Figure S7. Lithosphere-Asthenosphere Boundary. The depth is defined by the 1200°C isotherm, derived from the grids shown in Figure S6. (A) Shows the depth to the lithosphere-asthenosphere boundary as defined by the grids. (B) Shows depth to the lithosphere-asthenosphere boundary filtered to show long-wavelength component by removing contributions where the spherical harmonic coefficient l is larger than 60.

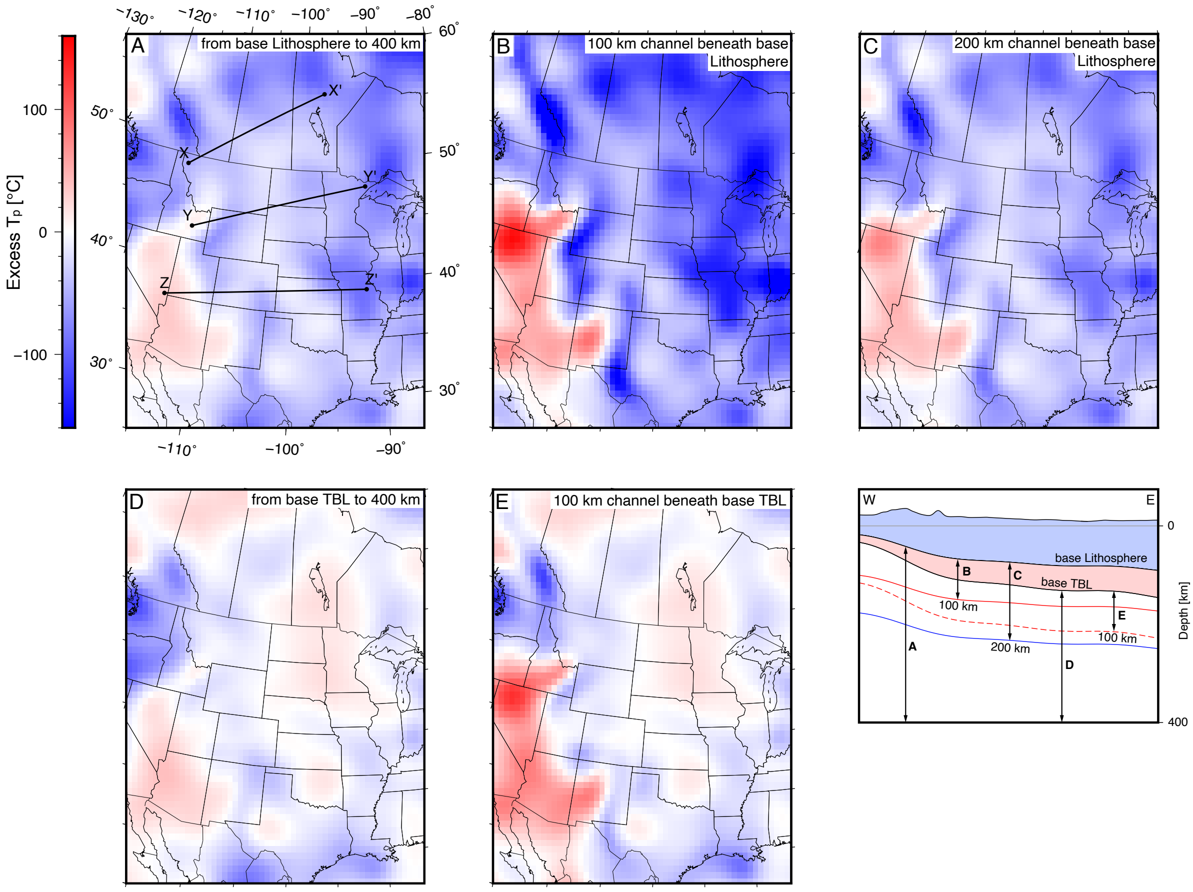

Figure S8. Excess asthenospheric temperatures. Mean excess potential temperatures from (A) base of the lithosphere to a depth of 400 km beneath Earth's surface, (B) within a 100 km thick channel beneath the plate, (C) with a 200 km thick channel beneath the plate, (D) from the base of the thermal boundary layer to a compensation depth of 400 km, and (E) within a 100 km thick channel at the base of the thermal boundary layer. Reference potential temperature is 1333°C. Schematic diagram shows different depth definitions used to calculate excess potential temperature.

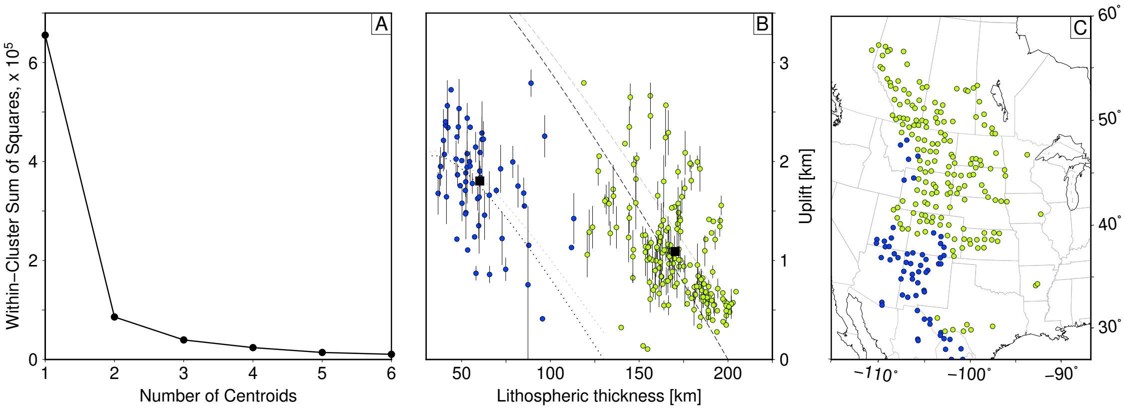

Figure S9. K-means clustering analysis of uplift as a function of lithospheric thickness. (A) Within cluster sum of squares for different numbers of clusters. Optimum number is 2, defined by the greatest reduction in variance. (B) K-means clusters for two centroids. Points are coloured by cluster. Black squares show centroids of clusters. Positions of centroids are consistent with (thermally equilibrated or disequilibrated) thinning of lithosphere with initial thicknesses of 130 km (black and grey dotted lines) or 200 km (back and grey dashed lines). Uplift data is spatially averaged in $1 \times 1^\circ$ bins. See body text of main manuscript for details.